Synthesis and Reactivity in Inorganic, Metal-Organic, and Nano-Metal Chemistry, 41:315–328, 2011

ISSN: 1553-3174 print / 1553-3182 online
DOI: 10.1080/15533174.2011.555865

Taylor & Francis
Taylor & Francis Group

Antibacterial, Spectral, and Thermal Aspects of Some [1,2,4-triazolo] [3,4-b][1,3,4]thiadiazine Based Heterochelates

Kaushal K. Oza, Darshan H. Jani, and Hasmukh S. Patel
Department of Chemistry, Sardar Patel University, Vallabh Vidyanagar, Gujarat, India

New ligands 5-((4-(3-(pyridine-4-yl)-7H-[1,2,4]triazolo[3,4-b][1,3,4]thiadiazine-6-yl)phenylamino)methyl)quinolin-8-ol (L_1) and 5-((3-(pyridine-4-yl)-7H-[1,2,4]triazolo[3,4-b][1,3,4]thiadiazine-6-ylamino)methyl)quinolin-8-ol (L_2) have been synthesized. The obtained ligands were characterized by ^{1}H NMR, ^{13}C NMR, and IR spectroscopic techniques, and reacted with transition metal salts to afford metal containing heterochelates. The structures of the synthesized heterochelates were characterized using elemental analyses, infrared spectra, electronic spectra, magnetic measurements, FAB mass spectrum, and thermo gravimetric analyses. The kinetic parameters, such as order of reaction (n) and the energy of activation (Ea), are reported using the Freeman–Carroll method. Ligands and heterochelates were also screened for their *in vitro* antibacterial activity.

Keywords 8-hyrdroxy quinoline, *in vitro* antibacterial activity, spectroscopy studies, thermal studies, thiadiazine

INTRODUCTION

In recent decades, the construction of metal–organic coordination architectures has witnessed tremendous growth because of their intriguing structures and potential properties.[1–4] Thiadiazines are efficient antibacterial and antifungal compounds,[5] and their use in the treatments of the bacterial helicobacter pylori and as reverse transcriptase inhibitors of the human immunodeficiency virus have been reported.[6,7] It was reported that the [1,2,4]triazolo[3,4-b][1,3,4]thiadiazines possess antimicrobial activity.[8] The [1,2,4] triazoles are known for their broad spectrum of biological activities and many other uses.[9–13] The synthesis of triazoles fused to another heterocyclic ring has attracted particular attention due to their diverse applications as antibacterial, antidepressant, antiviral, antitumoral, and anti-inflammatory agents, pesticides, herbicides, lubricant, and analytical reagents.[14,15] A number of triazoles fused to thiadiazines or thiadiazoles are incorporated into a wide variety of therapeutically important compounds possessing a broad spectrum of biological activities.[15–18] Hydroxyquinoline is a privileged structural moiety observed in many biologically active natural products, and is used as the source for many drugs diversely prescribed among a wide range of pathologies including neurodegenerative diseases,[19] parasitic amoebic dysentery disease,[20] and herpes viral diseases.[21] More specifically, 8-hydroxyquinoline moiety has been mostly used for its capacity to strongly chelate metal ions, particularly Cu^{+2} and Zn^{+2}.[22] 5-chlromethyl-8-quinolinol (CMQ) can be synthesized facilely and studied extensively.[23] From our lab, it was previously reported that CMQ clubbed benzotriazole derivatives and its metal chelates give enhanced antimicrobial activity.[24] Chelating ligands containing O and N donor atoms show broad biological activity and are of special interest because of the variety of ways in which they are bonded to metal ions.[25] The presence of transition metals in human blood plasma indicates their importance in the mechanism for accumulated storage and transport of transition metals in living organisms.[26] Transition metals play a key role in biological systems such as cell division, respiration, nitrogen fixation, and photosynthesis.[26]

Looking to pharmaceutically importance of thiadiazine and CMQ, the authors decided to synthesize ligand containing thiadiazine and CMQ in one molecule. They may afford the compound having not only the metal gripping potentiality, but may also have good biological efficiency. Hence, the present article describe the synthesis and characterization of a novel heterochelates, with Cu^{+2}, Co^{+2}, Ni^{+2}, Mn^{+2} and Zn^{+2} metal ions.

MATERIALS AND METHODS

Materials

The chemicals used for synthesis purpose were all of analytical grade, such as isoniazide, 8-hydroxy quinoline (purchased

Received 30 July 2010; accepted 1 October 2010.
The authors express gratitude to Department of Chemistry, Sardar Patel University, Vallabh Vidyanagar, India for providing laboratory facilities. Analytical facilities provided by the SAIF, Central Drug Research Institute, Lucknow, India. One of the authors, Kaushal K. Oza, is thankful to UGC New Delhi for providing scholarship.
Address correspondence to Hasmukh S. Patel, Department of Chemistry, Sardar Patel University, Vallabh Vidyanagar-388120, Gujarat, India. E-mail: drhspatel786@yahoo.com

from local market), Luria broth and agar-agar (from SRL, India), metal(II)-salts (chloride/nitrate/sulfate) of Mn(II), Co(II), Ni(II), Cu(II), and Zn(II) were used in their hydrated form. Silica gel F254 thin-layer chromatographic plates of size 20 × 20 cm were purchased from the E. Merck (India) Limited, Mumbai and used for purity evaluation. The organic solvents were purified by the recommended method.[27]

Instruments

The contents of carbon, hydrogen and nitrogen were analyzed with a Perkin Elmer, USA 2400-II CHN analyzer. The metal contents of the heterochelates were analyzed by EDTA titration after decomposing the organic matter with a mixture of concentrated $HClO_4$, H_2SO_4 and HNO_3 (1: 1.5: 2.5).[28] The melting points were checked by standard open capillary method and were uncorrected. Infrared spectra (4000–400 cm^{-1}) were recorded on Nicolet-400D spectrophotometer using KBr pellets. ^{1}H-NMR and ^{13}C-NMR spectra were recorded on a model Advance 400 Bruker FT-NMR instrument and DMSO-d_6 used as a solvent. The FAB mass spectrum of the heterochelate was recorded at SAIF, CDRI, Lucknow with Jeol SX-102/DA-6000 mass spectrometer. The magnetic moments were obtained by Gouy's method using mercury tetrathiocyanato cobaltate (II) as a calibrant (g = 16.44 × 10−6 c.g.s. units at 20°C). Diamagnetic corrections were made using Pascal's constant. The reflectance spectra of the ligands and their heterochelates were recorded in the range 1700–350 nm (as MgO disks) on a Beckman DK-2A spectrophotometer. A simultaneous • TG/DTG was obtained by a model 5000/2960 SDT, TA Instruments, USA. The experiments were performed in an N_2 atmosphere at a heating rate of 10°C min^{-1} in the temperature range 50–800°C, using an Al_2O_3 crucible. The sample sizes are ranged in mass from 5 to 8 mg.

Synthesis of Ligand

The uninegative bidentate ligands L_1 and L_2 were synthesized by condensation of 5-chloromethyl-8-hydroxyquinoline hydrochloride (CMQ) and 4-(3-(pyridine-4-yl)-7H-[1,2,4] triazolo[3,4-b][1,3,4]thiadiazine-6-yl)aniline and 3-(pyridine-4-yl)-7H-[1,2,4]triazolo[3,4-b][1,3,4]thiadiazine-6-amine, respectively. CMQ was prepared and used as starting materials for the synthesis of novel ligands L_1 and L_2 by slight modification of the method reported in the literature,[23] while metal(II) heterochelates of L_1 and L_2 were synthesized by a subsequently reported method.[29]

5-((4-(3-(pyridine-4-yl)-7H-[1,2,4]triazolo[3,4-b][1,3,4] thiadiazine-6-yl)phenylamino) methyl)quinolin-8-ol (L_1)

4-amino-5-(pyridine-4-yl)-4H-1,2,4-triazole-3-thiol was prepared according to reported method.[30] A mixture of N-(4-(2-chloroacetyl)phenyl)acetamide (100 mmol) and 4-amino-5-(pyridine-4-yl)-4H-1,2,4-triazole-3-thiol (100 mmol) and sodium acetate (250 mmol) in absolute ethanol was refluxed for 2 h. After cooling, the solvent was removed under vacuum and the precipitate formed was filtered, then washed with water. Dried crude product was taken up with conc. HCl and was refluxed for 2 h. After cooling in an ice bath, the mixture was neutralized with dilute alkali. The solid (4-(3-(pyridine-4-yl)-7H-[1,2,4]triazolo[3,4-b][1,3,4]thiadiazine-6-yl)aniline) obtained was filtered off and air dried. To the mixture of 4-(3-(pyridine-4-yl)-7H-[1,2,4]triazolo[3,4-b][1,3,4]thiadiazine-6-yl)aniline (8.00 g, 26.00 mmol) and triethylamine (8.18 g, 80.8 mmol) in dry pyridine (40 ml), CMQ (6.20 g, 26.90 mmol) was added with continuous stirring. The contents were refluxed for 150 min. The completion of the reaction was confirmed by TLC. The excess of pyridine was distilled off and the residue was poured into the ice-cold water to yield a light green product, which was filtered and washed with hot water and then dried over a vacuum desiccator. Yield, 71%; m.p., 183–185°C. Found (%): C, 64.48, H, 4.12, N, 21.00. $C_{25}H_{19}N_7OS$ (465.00) requires (%): C, 64.51, H, 4.08, N, 21.07. IR: 3293 (O—H), 1642 (C=N), 1502 (Ar C=C), 3310, 3140 (N—H), 1010 (N—N), 689 (C—S—C) ; ^{1}H NMR: 9.82 (1H, s, protons —OH), 6.70-8.82 (13H, m, protons Ar), 6.50 (1H, t, —N—H), 4.33 (2H, s, protons S—CH_2), 4.25 (2H, s, protons —CH_2); ^{13}C NMR: 156.68, 153.82, 153.52, 150.79, 149.48, 148.56, 144.43, 138.98, 136.49, 133.81, 130.04, 129.27, 127.98, 122.24, 121.68, 119.36, 113.96, 111.77, 45.00, 22.69.

5-((3-(pyridine-4-yl)-7H-[1,2,4]triazolo[3,4-b][1,3,4] thiadiazine-6-ylamino)methyl) quinolin-8-ol (L_2)

A mixture of 4-amino-5-(pyridine-4-yl)-4H-1,2,4-triazole-3-thiol (100 mmol), chloroacetonitrile (100 mmol) and sodium acetate (490 mmol) in ethanol was heated under reflux for 6 h. After cooling, the solvent was removed under reduced pressure and the solid product (3-(pyridine-4-yl)-7H-[1,2,4]triazolo[3,4-b][1,3,4]thiadiazine-6-amine) formed was washed with water and air dried. To the mixture of 3-(pyridine-4-yl)-7H-[1,2,4]triazolo[3,4-b][1,3,4]thiadiazine-6-amine (6.03 g, 26.00 mmol) and triethylamine (8.18 g, 80.8 mmol) in dry pyridine (40 ml), CMQ (6.20 g, 26.90 mmol) was added with continuous stirring. The contents were refluxed for 90 min. The completion of the reaction was confirmed by TLC. The excess of pyridine was distilled off and the residue was poured into the ice-cold water to yield a light green product which was filtered and washed with hot water and then dried over a vacuum desiccator. Yield, 73%; m.p., 171–173°C. Found (%): C, 58.60, H, 3.89, N, 25.21. $C_{19}H_{15}N_7OS$ (389.00) requires (%): C, 58.61, H, 3.85, N, 25.19. IR: 3286 (O—H), 1640 (C=N), 1510 (Ar C=C), 3312, 3132 (N—H), 1017 (N—N), 690 (C—S—C) ; ^{1}H NMR: 9.89 (1H, s, protons —OH), 6.72-8.80 (9H, m, protons Ar), 6.53 (1H, t, —N—H), 4.32 (2H, s, protons S—CH_2), 4.20 (2H, s, protons —CH_2); ^{13}C NMR: 156.80, 153.77, 152.51, 149.12, 148.32, 143.98, 138.30, 136.40, 133.80, 129.20, 127.98, 121.20, 119.30, 118.20, 111.70, 44.00, 22.60.

General Procedure for the Synthesis of Heterochelates

A warm solution of metal(II) salt (2.5 mmol) in 50% aqueous formic acid (2.5 ml) was added drop by drop with continuous stirring to previously warmed solution of ligand (5 mmol, 2 equivs) in 20% aqueous formic acid solution (20 ml). With the proper adjustment of the pH (6–7) with 50% NH_4OH, the resultant mixture was further digested in a water bath for 4–5 h and centrifuged. The suspended solid complex was allowed to settle and collected by filtration, washed with sufficient quantity of distilled water and then with a little hot ethanol and acetonitrile, then dried in vacuum desiccators over anhydrous calcium chloride. The physical data of ligand and heterochelates are shown in Table 1.

Bio Assay: Zone of Inhibition Technique

Preparation of Stock Solution

A stock solution of 10 mg ml^{-1} was made by dissolving compound in minimum amount of DMSO and making it up to the mark with double distilled water.

Preparation of Agar Plates

The media was made up by dissolving bacteriological agar (20 g) and Luria broth (20 g) (SRL, India) in 1 l distilled water. The mixture was autoclave for 15 min at 120°C and then dispensed into sterilized Petri dishes, allowed to solidify, and then used for inoculation.

Procedure of Inoculation

The target microorganism cultures were prepared separately in 15 ml of liquid Luria broth medium for activation. Inoculation was done with the help of micropipette with sterilized tips; 100 μl of activated strain was placed onto the surface of an agar plate, and spread evenly over the surface by means of a sterile, bent glass rod. Then two wells having diameter of 10 mm were made using a sterilized borer in each plate.

Application of Disks

Sterilized stock solutions (10 mg ml^{-1}) were used for the application in the well of earlier inoculated agar plates. When the disks were applied, they were incubated at 30°C (Gram-positive) and 37°C (Gram-negative) for 24 h. The zone of inhibition was then measured (in mm) around the disk. The control experiments were performed with only the equivalent volume of solvents without added test compounds and the zone of inhibitions was measured (in mm). All experiments were performed in triplicate, and ciprofloxacin was used as the standard drug.[31]

RESULTS AND DISCUSSION

5-Chloromethyl-8-hydroxyquinoline hydrochloride was prepared by chloromethylation of 8-hydroxyquinoline. Considerable difficulties were faced while obtaining high purity of CMQ even after washing the crude product with concentrated hydrochloric acid and acetone, which may have been caused by incomplete removal of 8-hydroxyquinoline. The possibility of substitution reaction during the crystallization with protic solvent was prevented by avoiding the use of inorganic base catalyst such as sodium/potassium bicarbonate, sodium/potassium hydrogen carbonate, and sodium hydroxide. An earlier report shows resultant slow reaction or presence of 5-hydroxymethyl-8-hydroxyquinoline in quantitative yield.[32] To overcome such discrepancies, triethylamine (TEA) was used as scavenger while reacting CMQ with 4-(3-(pyridine-4-yl)-7H-[1,2,4]triazolo[3,4-b][1,3,4]thiadiazine-6-yl)aniline and 3-(pyridine-4-yl)-7H-[1,2,4]triazolo[3,4-b][1,3,4]thiadiazine-6-amine to afford good yield. The synthesized novel ligands L_1 and L_2appear as light green crystals. It has partial solubility in acetone, methanol, ethanol, and acetonitrile, while being soluble in polar a protic solvents like dimethylformamide (DMF), dimethylsulfoxide (DMSO), organic acids, and pyridine. All the $[M(II)(L_1)_2(H_2O)_2]$ and $[M(II)(L_2)_2(H_2O)_2]$ had characteristic color, are stable in air, and practically insoluble in water, ethanol, methanol, chloroform, and hexane.

IR Spectra

The important infrared spectral bands and their tentative assignments for the synthesized heterochelates were recorded as KBr disks and are summarized in Table 2. In the 8-hydroxyquinoline complexes of divalent metals, the υ(C—O), appeared at 1120 cm^{-1} region and the position of the band slightly varies with the metal.[33] The υ(C—O), observed in the ligands molecule at 1082(L_1),1089(L_2) cm^{-1}, shifted to higher frequencies in all the hetero chelates, giving a strong absorption band at 1159–1189 cm^{-1}. This clearly indicates the coordination of 8-hydroxyquinoline in these complexes. The broad band at 3293(L_1), 3287 (L_2) cm^{-1} observed in the case of ligands was shifted in all heterochelates at ~3321 cm^{-1}, which was attributed to υ(O—H) of coordinated water molecule. In the investigated heterochelates, the bands observed in the region 3311–3331, 1272–1293, 866–879, and 708–715 cm^{-1} are attributed to —OH stretching, bending, rocking and wagging vibrations, respectively, due to the presence of water molecules. The presence of rocking band indicates the coordination nature of the water molecule.[34] Coordinated water were further supported by TG analysis. The υ(C═N) observed in the ligands and heterochelates at ~1642 cm^{-1}. The υ(N—H) observed at ~3310, ~3140 in the ligands and heterochelates. The υ(N—N) observed at ~1010, υ(C—S—C) at ~689, and which were attributed to thiadiazine ring in ligands and heterochelates.[35]

In the far-IR region, two new bands at ~504 and ~531 cm^{-1} in the heterochelates were assigned to υ(M—O) and υ(M—N), respectively.[36] All of these data confirm the fact that ligands $L_1$and L_2 behaves as uninegative bidentate.

^{1}H- and ^{13}C-NMR Spectra

Structural analysis of the ligands were carried out with the help of ^{1}H- and ^{13}C-NMR using DMSO-d_6 at room

TABLE 1
Analytical and physical data of the ligands and its heterochelate

Compounds	Formula weight (g mol^{-1})	Color (yield%)	Melting point (°C)	Analysis (%) calcd. (found)				μeff[a] (B.M)
				C	H	N	M	
L_1 $C_{25}H_{19}N_7OS$	465	Light green (71)	183–185	64.51 (64.48)	4.08 (4.12)	21.07 (21.00)	—	—
L_2 $C_{19}H_{15}N_7OS$	389	Light green (73)	171–173	58.61 (58.60)	3.85 (3.89)	25.19 (25.21)	—	—
$[Cu(L_1)_2(H_2O)_2]$ (1) Cu $C_{50}H_{40}N_{14}O_4S_2$	1027.21	Green (79)	>300	58.38 (58.40)	3.92 (3.96)	19.06 (19.10)	6.18 (6.20)	2.1
$[Co(L_1)_2(H_2O)_2]$ (2) Co $C_{50}H_{40}N_{14}O_4S_2$	1022.93	Brown (76)	>300	58.65 (58.61)	3.91 (3.98)	19.16 (19.12)	5.76 (5.75)	3.6
$[Ni(L_1)_2(H_2O)_2]$ (3) Ni $C_{50}H_{40}N_{14}O_4S_2$	1022.71	Green (73)	>300	58.66 (58.67)	3.91 (3.95)	19.16 (19.20)	5.74 (5.75)	3.2
$[Mn(L_1)_2(H_2O)_2]$ (4) Mn $C_{50}H_{40}N_{14}O_4S_2$	1018.94	Light green (80)	>300	58.88 (58.90)	3.92 (3.84)	19.23 (19.20)	5.39 (5.40)	5.7
$[Zn(L_1)_2(H_2O)_2]$ (5) Zn $C_{50}H_{40}N_{14}O_4S_2$	1029.37	Yellowish Green (73)	>300	58.28 (58.26)	3.88 (3.80)	19.64 (19.61)	6.35 (6.32)	D
$[Cu(L_2)_2(H_2O)_2]$ (6) Cu $C_{38}H_{32}N_{14}O_4S_2$	875.54	Green (81)	>300	52.08 (52.05)	3.65 (3.69)	22.38 (22.42)	7.25 (7.23)	2.0
$[Co(L_2)_2(H_2O)_2]$ (7) Co $C_{38}H_{32}N_{14}O_4S_2$	870.93	Brown (84)	>300	52.35 (52.31)	3.67 (3.76)	22.50 (22.54)	6.76 (6.72)	3.3
$[Ni(L_2)_2(H_2O)_2]$ (8) Ni $C_{38}H_{32}N_{14}O_4S_2$	870.71	Light Green (75)	>300	52.37 (52.33)	3.67 (3.72)	22.51 (22.52)	6.71 (6.70)	3.2
$[Mn(L_2)_2(H_2O)_2]$ (9) Mn $C_{38}H_{32}N_{14}O_4S_2$	866.94	Light green (79)	>300	52.59 (52.56)	3.69 (3.62)	22.60 (22.56)	6.33 (6.35)	5.5
$[Zn(L_2)_2(H_2O)_2]$ (10) Zn $C_{38}H_{32}N_{14}O_4S_2$	877.37	Yellowish Green (81)	>300	51.97 (51.98)	3.64 (3.68)	22.33 (22.36)	7.45 (7.41)	D

TABLE 2
The characteristic IR bands of ligands and their heterochelates

Compounds	υ(O–H) cm^{-1}	υ(C=N) cm^{-1}	υ(C–S–C) cm^{-1}	υ(C–O) cm^{-1}	υ(N–N) cm^{-1}	υ(M–O) cm^{-1}	υ(M–N) cm^{-1}
L_1	3293 (br)	1642 (w)	689 (s)	1082 (m)	1010 (m)	—	—
L_2	3287 (br)	1648 (w)	690 (s)	1089 (m)	1018 (m)	—	—
1	3311 (br)	1643 (w)	682 (s)	1159 (m)	1020 (m)	504	531
2	3323 (br)	1642 (w)	694 (s)	1189 (m)	1017 (m)	507	537
3	3331 (br)	1637 (w)	685 (s)	1177 (m)	1004 (m)	509	547
4	3318 (br)	1640 (w)	681 (s)	1164 (m)	1009 (m)	510	549
5	3323 (br)	1639 (w)	694 (s)	1181 (m)	1013 (m)	519	534
6	3327 (br)	1647 (w)	681 (s)	1167 (m)	1014 (m)	510	539
7	3323 (br)	1639 (w)	684 (s)	1172 (m)	1008 (m)	508	532
8	3329 (br)	1643 (w)	691 (s)	1179 (m)	1012 (m)	517	534
9	3317 (br)	1632 (w)	682 (s)	1183 (m)	1019 (m)	503	543
10	3319 (br)	1642 (w	693 (s)	1188 (m)	1017 (m)	507	546

s=strong, m=medium, w=weak, br=broad, m= metal

temperature. The data are presented in the Experimental section. In the case of ^{1}H-NMR spectra for the ligands, one broad singlet equivalent to one proton was observed at 9.82 (L_1), 9.89 (L_2) δ ppm corresponding to O—H group.[37,38] This signal disappeared when a D_2O exchange experiment was carried out. For the ligand L_1 in the region of 6.70–8.82 δ ppm, multiplate were observed, equivalent to thirteen protons corresponding to aromatic protons. For the ligand L_2 in the region of 6.72–8.80 δ ppm, multiplate were observed, equivalent to nine protons corresponding to aromatic protons. At 6.50 (L_1), 6.53 (L_2) δ ppm triplet was observed, equivalent to one proton corresponding to N—H. At 4.33 (L_1), 4.32 (L_2) δ ppm singlet was observed, equivalent to two protons corresponding to S—$CH_2$of thiadiazine ring. Another singlet was observed, equivalent to two protons corresponding to —CH_2 at 4.25 (L_1), 4.20 (L_2) δ ppm. By comparing the ^{1}H-NMR data of the ligands and the Zn(II) heterochelate, it was concluded that the signal for —OH proton disappears in case of Zn(II) heterochelate. Disappearance of this signal in case of Zn(II) heterochelate is attributed to loss of proton due to coordination of oxygen atom

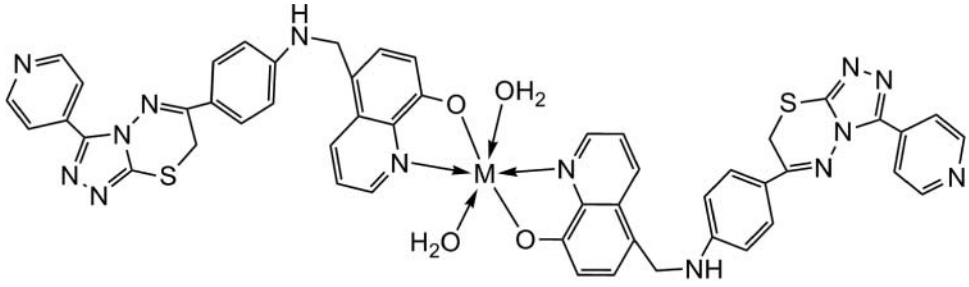

Where M= Cu^{+2}, Co^{+2}, Ni^{+2}, Mn^{+2}, Zn^{+2} For compounds 1,2,3,4,5

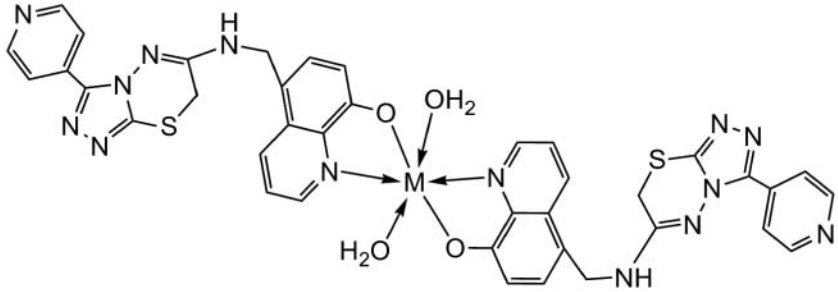

Where M= Cu^{+2}, Co^{+2}, Ni^{+2}, Mn^{+2}, Zn^{+2} For compounds 6,7,8,9,10

FIG. 1. Proposed structures of heterochelates.

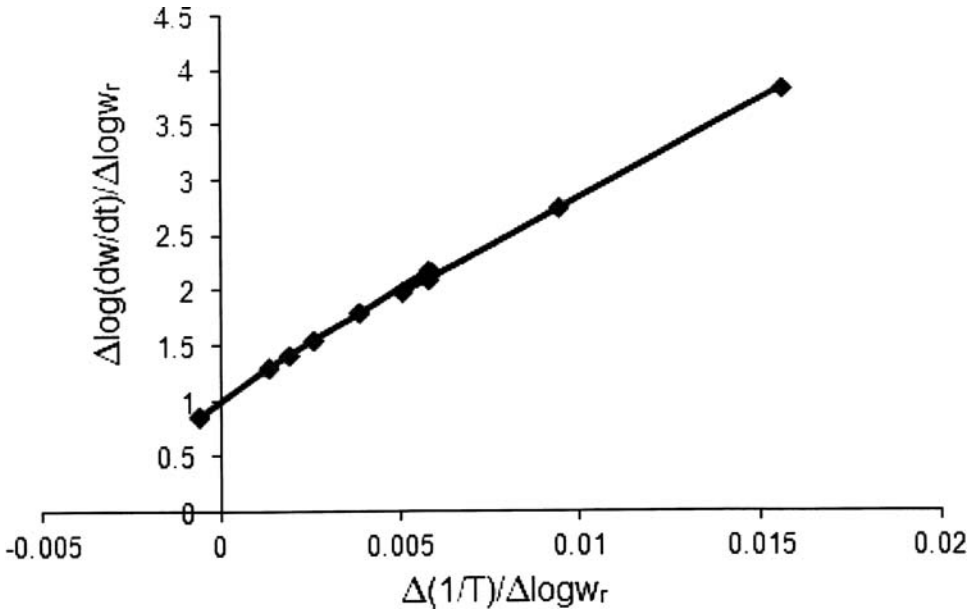

FIG. 2. Freeman-Carroll plot for the heterochelate $[Cu(L_1)2(H_2O)_2]$.

with metal ion.[39] The signal for adjacent proton attached to N of quinoline appeared at very low magnetic field compared with that of ligand, suggesting the involvement of N in the heterochelate formation. In the ^{1}H NMR spectra of Zn(II) heterochelates, all other signals that remain unaltered as compared with ligands suggest non involvement of this groups.

In ^{13}C-NMR spectra of L_1, peaks observed at 156.68, 153.82, 153.52, 150.79, 149.48, 148.56, 144.43, 138.98, 136.49, 133.81, 130.04, 129.27, 127.98, 122.24, 121.68, 119.36, 113.96, and 111.77 δ ppm were assigned to aromatic carbons. Aliphatic carbons were observed at 45.00, 22.69 ppm. In ^{13}C-NMR spectra of L_2, peaks observed at 156.80, 153.77, 152.51, 149.12, 148.32, 143.98, 138.30, 136.40, 133.80, 129.20, 127.98, 121.20, 119.30, 118.20, and 111.70 δ ppm were assigned to aromatic carbons. Aliphatic carbons were observed at 44.00, 22.60 ppm.

Diffuse Electronic Spectral and Magnetic Properties Data

The diffuse electronic spectra of $[Cu(L_1)_2(H_2O)_2]$, $[Cu(L_2)_2(H_2O)_2]$ exhibited two bands, at 26238 cm^{-1} and 26247

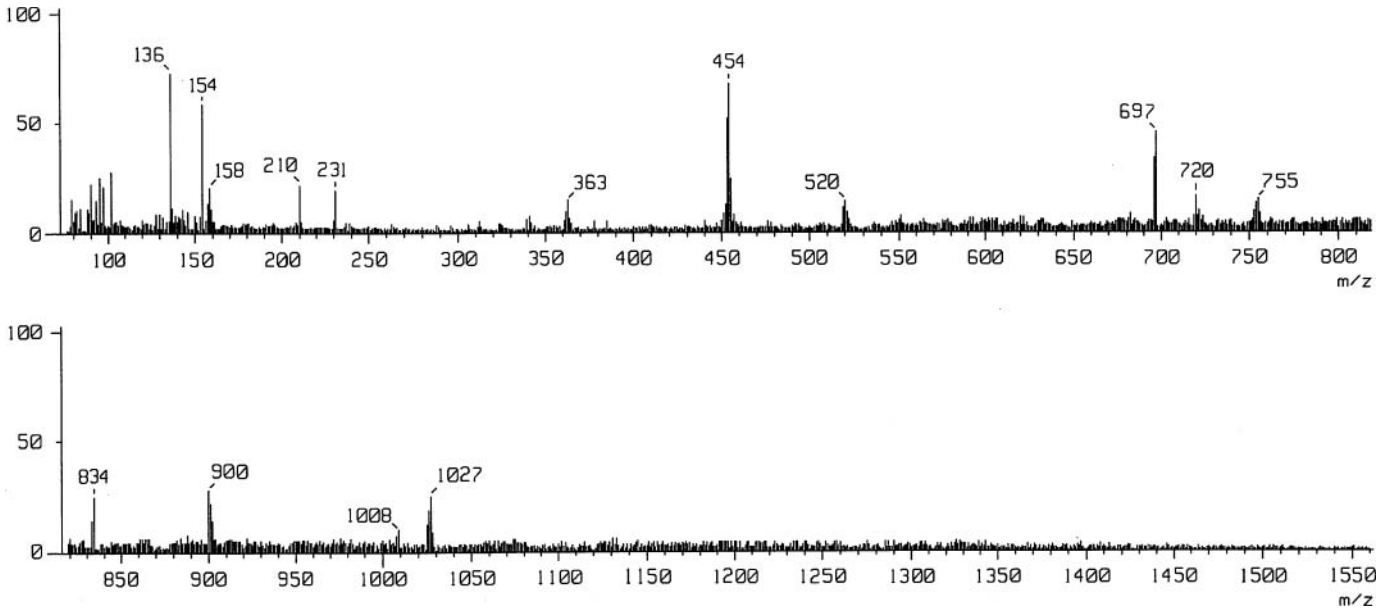

FIG. 3. FAB Mass spectrum for the heterochelate $[Cu(L_1)2(H_2O)_2]$.

TABLE 3
Thermoanalytical results (TG, DTG) of the heterochelates

Compounds	TG range/°C	DTG max/°C	Mass loss % Obs.(calcd.)	Assignment
1	120–210	189	3.51(3.50)	Loss of two coordinated water molecules
	210–453	293	50.15	Removal of some part of ligand
	453–800	679	40.16	Removal of remaining part of ligand leaving CuO residue.
2	134–205	187	3.49(3.51)	Loss of two coordinated water molecules
	205–443	—	52.55	Removal of some part of ligand
	443–800	648	38.16	Removal of remaining part of ligand leaving CoO residue
3	124–209	176	3.50(3.52)	Loss of two coordinated water molecules
	209–449	310	55.77	Removal of some part of ligand
	449–800	603	34.96	Removal of remaining part of ligand leaving NiO residue
4	125–200	183	3.55(3.53)	Loss of two coordinated water molecules
	200–451	402	49.71	Removal of some part of ligand
	451–800	697	41.36	Removal of remaining part of ligand leaving MnO residue
5	122–205	151	3.47(3.49)	Loss of two coordinated water molecules
	205–442	—	52.56	Removal of some part of ligand
	442–800	689	37.59	Removal of remaining part of ligand leaving ZnO residue
6	125–189	154	4.14(4.11)	Loss of two coordinated water molecules
	189–410	317	49.77	Removal of some part of ligand
	410–800	543	38.86	Removal of remaining part of ligand leaving CuO residue.
7	127–183	162	4.12(4.13)	Loss of two coordinated water molecules
	183–403	298	51.54	Removal of some part of ligand
	403–800	678	37.56	Removal of remaining part of ligand leaving CoO residue
8	117–185	169	4.15(4.13)	Loss of two coordinated water molecules
	185–413	323	49.93	Removal of some part of ligand
	413–800	643	39.19	Removal of remaining part of ligand leaving NiO residue
9	118–191	149	4.13(4.15)	Loss of two coordinated water molecules
	191–407	353	52.56	Removal of some part of ligand
	408–800	—	36.95	Removal of remaining part of ligand leaving MnO residue
10	128–192	178	4.12(4.10)	Loss of two coordinated water molecules
	192–412	—	48.63	Removal of some part of ligand
	412–800	590	39.81	Removal of remaining part of ligand leaving ZnO residue

cm^{-1}, respectively, due to charge transfer and a broad band having maxima at 1558 $cm^{-1}$and 1567 cm^{-1}, respectively, due to the $^2Eg \rightarrow {}^2T_{2g}$ transition. The broadening of the signal might be due to Jahn–Teller distortion. The absorption bands of the diffuse electronic spectra and the value of their magnetic moment favor a tetragonally distorted octahedral geometry around Cu(II) ion.[40–42] $[Ni(L_1)_2(H_2O)_2]$, $[Ni(L_2)_2(H_2O)_2]$ showed three weak absorption bands at 9974, 16013, and 24464 cm^{-1}, 9969, 16000, and 24434 cm^{-1}, respectively, corresponding to the characteristic transitions $^3A_{2g} \rightarrow {}^3T_{2g}$, $^3A_{2g} \rightarrow {}^3T_{1g}(F)$, $^3A_{2g} \rightarrow {}^3T_{1g}(P)$. $[Co(L_1)_2(H_2O)_2]$, $[Co(L_2)_2(H_2O)_2]$ exhibited three absorption bands at 9828, 15481, and 22107 cm^{-1}, 9813, 15460, and 22110 cm^{-1}, respectively, due to $^4T_{1g}(F) \rightarrow {}^4T_{2g}(F)$, $^4T_{1g}(F) \rightarrow {}^4A_{2g}(F)$ and $^4T_{1g}(F) \rightarrow {}^4T_{1g}(P)$ transitions. The

TABLE 4
Thermodynamic data of the thermal decomposition of heterochelates

Compounds	TG range/°C	*Ea*/kJ mol^{-1}	*n*	*A*/s^{-1}	*S**/JK^{-1} mol^{-1}	*H**/kJ mol^{-1}	*G**/kJ mol^{-1}
1	120–210	11.55	0.99	9.46	−96.72	9.52	42.62
	210–453	13.36	1.00	1.65	−97.64	10.04	60.54
	453–800	14.25	0.98	0.89	−99.72	11.02	72.45
2	134–205	3.31	0.98	0.22	−100.05	0.76	32.66
	205–443	14.63	0.98	1.05	−99.00	9.79	66.57
	443–800	27.57	1.00	2.23	−97.01	20.41	102.84
3	124–209	3.09	1.00	0.05	−102.32	−0.22	42.32
	209–449	10.18	0.99	0.21	−100.24	5.43	61.84
	449–800	30.59	1.00	19.53	−95.86	25.08	89.26
4	125–200	3.11	1.00	0.11	−101.48	0.34	32.43
	200–451	6.08	1.00	0.10	−100.42	2.36	57.57
	451–800	33.69	0.98	8.25	−96.20	26.86	106.38
5	122–205	3.11	0.98	0.13	−100.11	0.23	39.34
	205–442	6.10	1.00	0.25	−99.24	2.24	58.89
	442–800	33.72	0.99	5.22	−95.86	26.75	94.26
6	125–189	11.54	0.99	9.43	−96.74	9.32	42.68
	189–410	13.35	0.98	1.68	−97.64	10.03	60.51
	410–800	14.26	1.00	0.81	−99.75	11.01	72.49
7	127–183	3.34	0.99	0.23	−100.10	0.74	32.61
	183–403	14.69	0.99	1.00	−99.03	9.72	66.53
	403–800	27.51	1.00	2.22	−97.00	20.44	102.74
8	117–185	3.10	0.99	0.04	−102.22	−0.21	42.31
	185–413	10.20	0.99	0.22	−100.44	5.47	61.86
	413–800	30.61	1.00	19.43	−95.76	25.07	89.22
9	118–191	3.19	1.00	0.19	−101.89	0.37	32.47
	191–407	6.12	0.98	0.18	−100.34	2.34	57.52
	408–800	33.72	1.00	8.24	−96.10	26.88	106.39
10	128–192	3.13	0.99	0.12	−100.21	0.24	39.33
	192–412	6.13	1.00	0.24	−99.14	2.21	58.87
	412–800	33.70	0.98	5.19	−95.36	26.65	94.23

absorption bands of the diffuse electronic spectra and values of their magnetic moments show an octahedral geometry around Ni(II) and Co(II) ions.[43,44] The spectra of $[Mn(L_1)_2(H_2O)_2]$, $[Mn(L_2)_2(H_2O)_2]$ showed weak bands at 16776, 18421, and 23807 cm^{-1}, 16766, 18431, and 23812 cm^{-1}, respectively, assigned to the $^6A_{1g} \rightarrow {}^4T_{1g}$, $^6A_{1g} \rightarrow {}^4T_{2g}$, $^6A_{1g} \rightarrow {}^4A_{1g}$, ^{4}Eg transitions and their magnetic moment values suggest an octahedral geometry for the Mn(II) ion. As the spectrum of $[Zn(L_1)_2(H_2O)_2]$, $[Zn(L_2)_2(H_2O)_2]$ was not well resolved, it was not well interpreted, but its magnetic moment value shows that it is diamagnetic in nature, as expected.[29] The results of the magnetic moment value (Table 1) were shown to have octahedral geometry for all the Hetero chelates. Hence, the observed values of magnetic moments and the electronic spectra of hetero chelates supported octahedral geometry for all the structures.[45] Probable structure of the complexes from the above analytical facts is given below in Figure 1.

Thermal Response of Synthesized Heterochelate

The thermal behavior of the heterochelates was determined using a 5000/2960 SDTA, TA instrument (USA) differential thermal analysis apparatus operating at a heating rate of 10°C per minute in the range of 50–800°C in N_2 atmosphere. Securitization of this data envisages that all heterochelates follows three-step thermal decomposition. Each decomposition process follows the trend given below in scheme. This process comprises of several stages. The method reported by Freeman–Carroll method [46] has been adopted. Plots of [Δlog(dw/dt)/Δlog wr] vs. [Δ(1/T)/Δlog wr] were linear for all of the decomposition steps. The energy of activation Ea was calculated from the slopes of these plots for a particular stage and the order of reactions (n) determined from the intercept, showing first order reaction over the entire range of decomposition for all of the heterochelates. A typical Freeman–Carroll plot for the thermal degradation of $[Cu(L_1)_2(H_2O)_2]$ is shown in Figure 2.

The thermal fragmentation scheme for heterochelates $[M(L_n)_2(H_2O)_2]$ is as shown in Scheme 1:

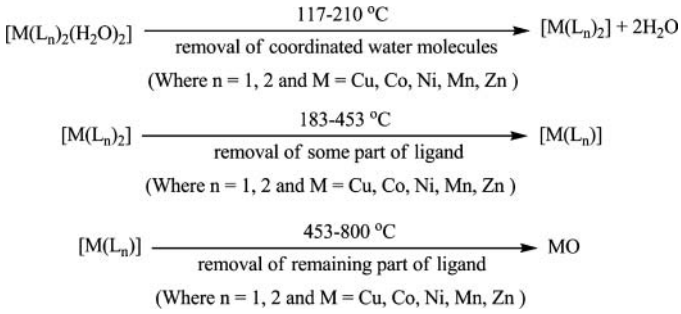

SCH. 1.

In the first decomposition step, the weight loss during 117–210°C corresponds to two coordinated water molecules. A loss in weight observed in the second step was corresponding to the decomposition and combustion of some part of ligand in the temperature range 183–453°C. The third subsequent stage for heterochelates shows the decomposition and combustion of remaining part of ligand. The removal of ligand undergoes decomposition forming MO as the final residue.

The thermodynamic activation parameters of the decomposition process of dehydrated heterochelates such as activation entropy (S*), pre-exponential factor (A), activation enthalpy (H*) and free energy of activation (G*), were calculated using the reported equations.[47] According to the kinetic data obtained from DTG curves, all the heterochelates have negative entropy, which indicates that the studied heterochelates have more ordered systems than reactants.[48] The kinetic parameters, especially energy of activation (Ea) is helpful in assigning the strength of the bonding of ligand moieties with the metal ion. The calculated Ea values of the investigated heterochelates for the degradation stage of ligand are in the range 3.09–33.72 kJ mol^{-1}. The relative high Ea value indicates that the ligand is strongly bonded to the metal ion.[49] From the above discussion, an octahedral geometry of the heterochelates can tentatively be assumed as shown in Figure 1. Thermoanalytical and thermodynamic data of heterochelates are reported in Tables 3 and 4, respectively.

FAB Mass Spectra

The recorded FAB mass spectrum (Figure 3) and the molecular ion peak for the heterochelate $[Cu(L_1)_2(H_2O)_2]$ were used to confirm the molecular formula. The proposed fragmentation pattern is shown in Scheme 2. The first peak at m/z 1027 represents the molecular ion peak of the heterochelate. Scheme 2 demonstrates the possible degradation pathway for the investigated heterochelate. The primary fragmentation of the heterochelate takes place due to the loss of one coordinated H_2O molecule from the species (a) to give species (b) with peak at m/z 1008. The species (b) further degrades to give species (c) with peak at m/z 834 with loss of one coordinate H_2O molecule and $-C_{10}H_8N_2$ moieties. Species (c) further degrades with the loss of $-C_4H_3N_4S$ moieties forming species (d) with a peak at m/z 697. Species (d) further degrades with loss of $-C_4H_3N_4S$ and $-C_7H_8N$ forming species (e). The sharp peak (base peak) observed at m/z 454 represents the stable species (e) with 99.0% abundance. Species (e) further degrades with loss of $-C_6H_6N$ forming species (f) at m/z 363. Species (f) further degrades with loss of $-C_9H_6N$ and CuO forming species (g).The measured molecular weights for all the suggested degradation steps were consistent with expected values.[50]

TABLE 5
In vitro activity data of ligands and heterochelates

Compounds	Zone of inhibition (mm)			
	Bacillus subtilis	*Staphylococcus aureus*	*Escherichia coli*	*Serratia marcescens*
Ciprofloxacin	33	39	38	44
L_1	11	13	14	12
L_2	12	09	08	10
1	30	36	33	36
2	19	21	18	20
3	21	25	26	26
4	15	17	11	19
5	18	16	20	15
6	29	32	31	32
7	13	19	21	18
8	19	22	28	24
9	18	15	18	13
10	17	20	21	16

Antimicrobial Screening

Zone of Inhibition

The increase in antimicrobial activity may be considered in light of Overtone's concept and Tweedy's chelation theory. According to Overtone's concept of cell permeability, the lipid membrane surrounding the cell favors the passage of lipid-soluble materials making the solubility an important factor controlling the antimicrobial activity. On chelation, the polarity of the metal ion will be reduced to a greater extent due to the overlap of the ligand orbital and partial sharing of the positive charge of the metal ion with donor groups. Further, it increases the delocalization of π-electrons over the whole chelate ring and enhances the lipophilicity of the heterochelates. The increased lipophilicity enhances the penetration of the heterochelates into lipid membranes and blocks the metal binding sites in the enzymes of microorganisms. These heterochelates also disturb the respiration process of the cell and block the synthesis of proteins, which actually restricts further growth of the organisms. Furthermore, the mode of action comprising the compounds may involve the formation of hydrogen bond through the azomethine/carbonyl/amine group with the active center of cell constituents and interferences are forced with the normal cell process.[31,51,52]

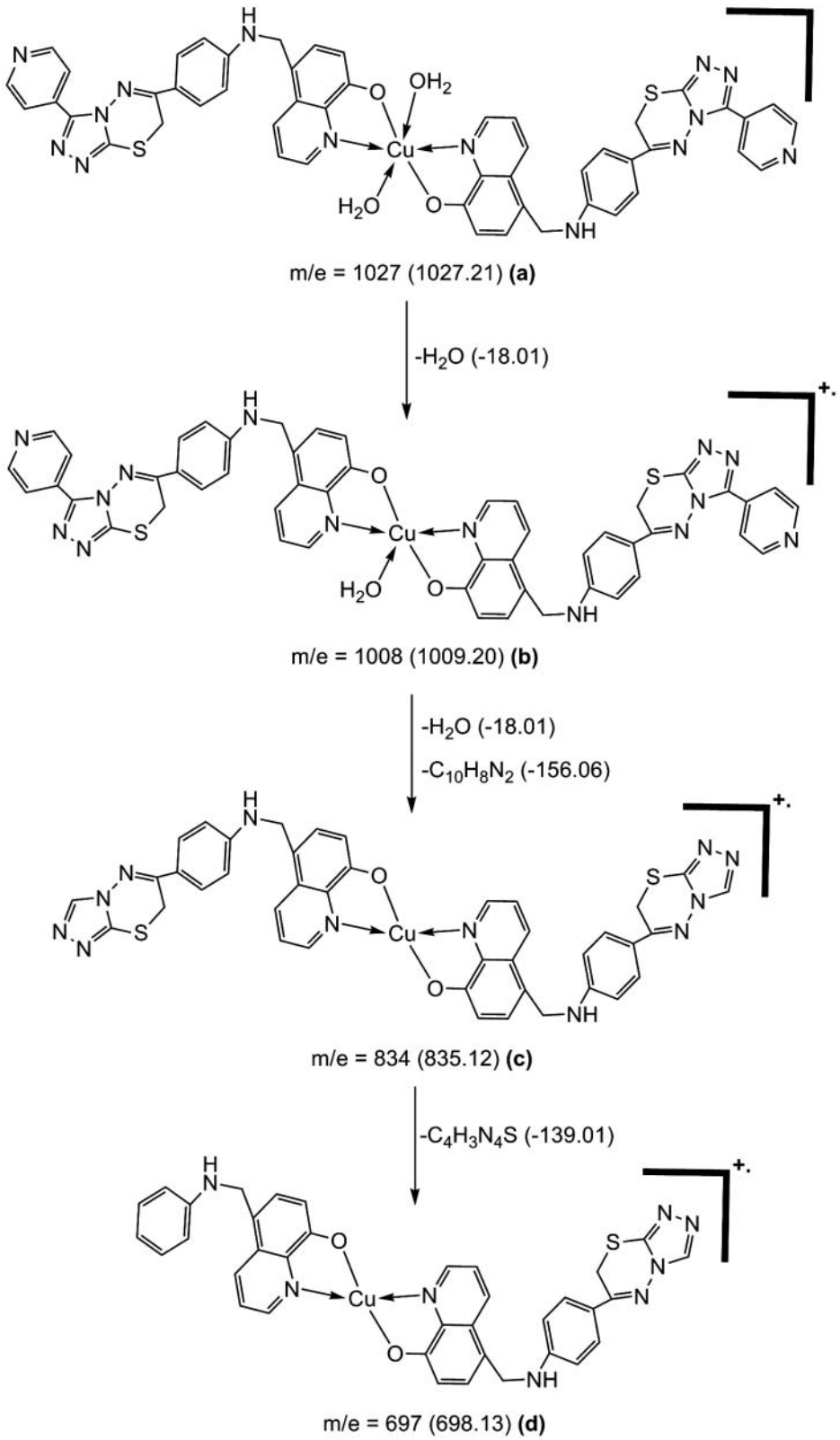

SCH. 2. The suggested fragmentation pattern of compound **1**.

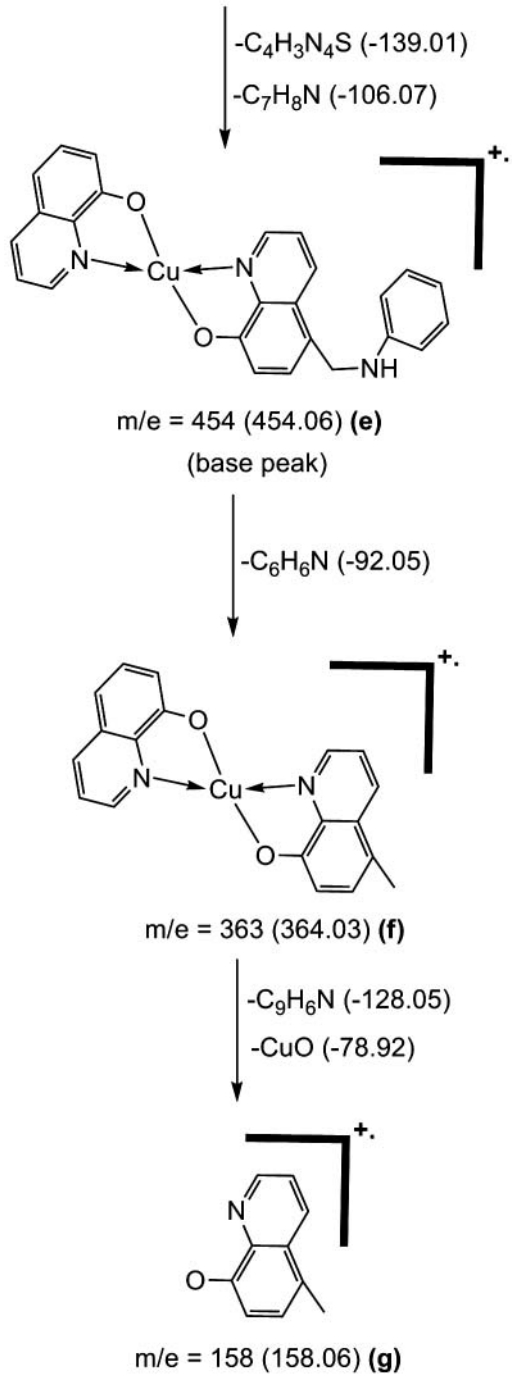

SCH. 2. (Continued)

It was observed that all the heterochelates were proven to be more potent bacteriostatic compared to ligands, while Cu(II) heterochelate is highly active against all the organism among the heterochelates of the respective metal. Heterochelates exhibit different characteristic properties, which depend on the metal ion to which they are bound, the nature of the metal as well as the type of ligand, etc. These heterochelates have found extensive applications in various fields of human interest. The nature of a coordination compound depends on the metal ion and the donor atoms, as well as on the structure of the ligand and the metal–ligand interaction.[53,54] Metal ions play a vital role in a vast number of different biological processes through co-enzymatic systems. The interaction of these ions with biologically active ligands, for instance in drugs, is a subject of great interest. Some

biologically active compounds act via chelation, but for most of them little is known about how metal coordination influences their activity. This may support the argument that some type of bimolecular binding to the metal ions or intercalation or electrostatic interactions causing the inhibition of biological synthesis and preventing the organisms from reproducing.[55] The strong antimicrobial activities of these compounds against tested organisms suggest further investigation on these compounds. The antimicrobial activity data of the compounds are summarized in Table 5.

CONCLUSIONS

The design and synthesis of ligands L_1 and L_2 have successfully been demonstrated by FT-IR, ^{1}H-NMR, and ^{13}C-NMR spectral studies. A series of some novel heterochelates was synthesized and characterized for their properties. All the products were screened for their bioassay. The heterochelates exhibited strong activities against two Gram-negative (*Escherichia coli, Serratia marcescens*) and two Gram-positive (*Staphylococcus aureus, Bacillus subtilis*) microorganisms. In comparison with the ligands, the heterochelates were more active against one or more bacterial strains, introducing a novel class of metal-based bactericidal agents. The information regarding geometrical confirmations concerning the structure of the heterochelates was obtained from their electronic and magnetic moment values. Magnetic moment measurements revealed high-spin, lacking exchange interactions for the heterochelates. From the overall information obtained, the heterochelates are supposed to be structurally arranged in octahedral geometry.

REFERENCES

1. (a) Ockwig, N.W.; Delgado-Friedrichs, O.; O'Keeffe, M.; Yaghi, O.M. Reticular chemistry: occurrence and taxonomy of nets and grammar for the design of frameworks. *Acc. Chem. Res.* **2005**, *38*, 176–182. (b) Kesanli, B.; Lin, W. Chiral porous coordination networks: rational design and applications in enantioselective processes. *Coord. Chem. Rev.* **2003**, *246*, 305–326. (c) Braga, D.; Grepioni, F.; Desiraju, G.R. Crystal engineering and organometallic architecture. *Chem. Rev.* **1998**, *98*, 1375–1405. (d) Miyasaka, H.; Matsumoto, N.; Okawa, H. N. Re.; Gallo, E.; Floriani, C. Complexes derived from the reaction of manganese(III) Schiff base complexes and hexacyanoferrate(III): Syntheses, multidimensional network structures, and magnetic properties. *J. Am. Chem. Soc.* **1996**, *118*, 981–994. (e) Kobayashi, H.; Tomita, H.; Naito, T.; Kobayashi, A.; Sakai, F.; Watanabe, T.; Cassoux, P. New BETS conductors with magnetic anions (BETS=bis(ethylenedithio)tetraselenafulvalene). *J. Am.Chem. Soc.* **1996**, *118*, 368.
2. (a) Seidel, S.R.; Stang, P. J. High-symmetry coordination cages via self-assembly. *Acc. Chem. Res.* **2002**, *35*, 972–983. (b) Rosi, N.L.; Kim, J.; Eddaoudi, M.; Chen, B.; O'Keeffe, M.; Yaghi, O.M. Rod packings and metal−organic frameworks constructed from rod-shaped secondary building units. *J. Am. Chem. Soc.* **2005**, *127*, 1504–1518. (c) Sato, O.; Iyoda, T.; Fujishima, A.; Hashimoto, K. Electrochemically tunable magnetic phase transition in a high-T_c chromium cyanide thin film. *Science* **1996**, *271*, 49–51. (d) Zaworotko, M. J. Nanoporous structures by design. *Angew. Chem., Int. Ed.* **2000**, *39*, 3052–3054. (e) Gardner, G.B.; Venkataraman, D.; Moore, J.S.; Lee, S. Spontaneous assembly of a hinged coordination network. *Nature* **1995**, *374*, 792–795. (f) Kou, H.Z.; Gao, S.; Zhang, J.; Wen, G.H.; Su, G.; Zheng, R.K.; Zhang, X.X. Unexpected assembly of a unique cyano-bridged three-dimensional Cu_3Cr_2 ferromagnet. *J. Am. Chem. Soc.* **2001**, *123*, 11809–11810.
3. (a) Blake, A.J.; Champness, N.R.; Hubberstey, P.; Li, W.S.; Withersby, M.A.; Schroder, M. Inorganic crystal engineering using self-assembly of tailored building-blocks. *Coord. Chem. Rev.* **1999**, *183*, 117–138. (b) Chui, S.S.Y.; Lo, S.M.F.; Charmant, J.P.H.; Orpen, A.G.; Williams, I.D. A chemically functionalizable nanoporous material $[Cu_3(TMA)_2(H_2O)_3]_n$ *Science* **1999**, *283*, 1148–1150. (c) Melcer, N.J.; Enright G.D.; Ripmeester J.A.; Shimizu G.K.H. The effects of anion variation and ligand derivatization on silver coordination networks based upon weaker interactions. *Inorg. Chem.* **2001**, *40*, 4641–4648. (d) Cao, R.; Sun, D.F.; Liang, Y.C.; Hong, M.C.; Tatsumi, K.; Shi, Q. Syntheses and characterizations of three-dimensional channel-like polymeric lanthanide complexes constructed by 1,2,4,5-benzenetetracarboxylic acid. *Inorg. Chem.* **2002**, *41*, 2087–2094. (e) Tong, M.L.; Wu, Y.M.; Ru, J.; Chen, X.M.; Chang, H.C.; Kitagawa, S. Pseudo-polyrotaxane and β-sheet. Layer-based three-dimensional coordination polymers constructed with silver salts and flexible pyridyl-type ligands. *Inorg. Chem.* **2002**, *41*, 4846–4848. (f) Wu, C.-D.; Lin W.-B. Highly porous, homochiral metal-organic frameworks: solvent-exchange-induced single-crystal to single-crystal transformations. *Angew. Chem., Int. Ed.* **2005**, *44*, 1958–1961.
4. (a) Wu, C.-D.; Hu, A.; Zhang L.; Lin W. A homochiral porous metal−organic framework for highly enantioselective heterogeneous asymmetric catalysis. *J. Am. Chem. Soc.* **2005**, *127*, 8940–8941. (b) Seo, J.S.; Whang, D.; Lee, H.; Jun, S.I.; Oh, J.; Jeon, Y.J.; Kimoon, K. A homochiral metal–organic porous material for enantioselective separation and catalysis. *Nature* **2000**, *404*, 982–986. (c) Ye, Q.; Li, Y.-H.; Song, Y.-M.; Huang, X.-F.; Xiong, R.-G.; Xue, Z. A second-order nonlinear optical material prepared through in situ hydrothermal ligand synthesis. *Inorg. Chem.* **2005**, *44*, 3618–3625.
5. El Bialy, S.A.A.; Abdelal A.M.; El, S.A.N.; Kheria, M.M. 2,3-bis(5-alkyl-2-thiono-1,3,5-thiadiazin-3-yl) propionic acid: One-pot domino synthesis and antimicrobial activity. *Arch. Der Pharm.* **2005**, *338*, 38–43.
6. Costin, J.C. Method and compostions for the control or the eradication of helicobacter pylori. *U.S. Patent.,* **2003**, *6*, 555, 534.
7. Witvrouw, M.; Arranz, M.E.; Pannecouque, C.; Declercq, R.; Jonckheere, H.; Schmit, J. C.; Vandamme, A. M.; Diaz, J. A.; Ingate, S. T.; Desmyter, J.; Esnouf, R.; VanMeervet, L.; Vega, S.; Balzarini, J.; DeClercq, E. 1,1,3-trioxo-2H,4H-thieno[3,4-e][1,2,4]thiadiazine (TTD) derivatives: a new class of nonnucleoside human immunodeficiency virus type 1 (HIV-1) Reverse transcriptase inhibitors with anti-HIV-1 activity. *Antimicrob. Agents Chemother*. **1998**, *42*, 618–623.
8. Demirbas, N.; Demirbas, A.; Karaoglu, S. A.; Celik, E. Synthesis and antimicrobial activities of some new [1,2,4]triazolo[3,4-b][1,3,4]thiadiazoles and [1,2,4]triazolo[3,4-b] [1,3,4]thiadiazines. *ARKIVOC* **2005**, *(i)*, 75–91.
9. Ghorab, M.M.; El-Sharief, A. MSh.; Ammar, Y.A.; Mohamed, Sh. I. Synthesis and antifungal activity of some new miscellaneous s-triazoles. Phosph. *Sulf., Silicon. and Relat. Elem.* **2001**, *173*, 223–233
10. Shi, H.; Wang, Z.; Shi, H. Synthesis of chiral fused heterocyclic compounds containing 1,2,4-triazole ring. *J. Heterocycl. Chem.* **2001**, *38*, 355–357.
11. Palaska, E.; Sahin, G.; Kelicen, P.; Durlu, N.T.; Altinok, G. Synthesis and anti-inflammatory activity of 1-acylthiosemicarbazides, 1,3,4-oxadiazoles, 1,3,4-thiadiazoles and 1,2,4-triazole-3-thiones. *Il Farmaco,* **2002**, *57*, 101–107.
12. Labanauskas, L.; Kalcas, V.; Udrenaite, E.; Gaidelis, P.; Brukstus, A.; Dauksas, V. Synthesis of 3-(3,4-dimethoxyphenyl)-1H-1,2,4-triazole-5-thiol and 2-amino-5-(3,4-dimethoxyphenyl)-1,3,4-thiadiazol derivatives exhibiting anti-inflammatory activity. *Pharmazie* **2001**, *56*, 617–619.
13. Foroumadi, A.; Mirzaei, M.; Shafiee, A. Antitubercular agents, I: Synthesis and antituberculosis activity of 2-aryl-1,3,4-thiadiazole derivatives. *Pharmazie*, **2001**, *56*, 610–612.

14. Holla, B.S.; Poorjary, N.K.; Rao, S.B.; Shivananda, M. K. New bis-aminomercaptotriazoles and bis-triazolothiadiazoles as possible anticancer agents. *Eur. J. Med. Chem.* **2002**, *37*, 511–517.
15. Holla, B.S.; Akberali, P.M.; Shivananda, M.K. Studies on nitrophenylfuran derivatives*[1]: Part XII. Synthesis, characterization, antibacterial and antiviral activities of some nitrophenylfurfurylidene-1,2,4-triazolo[3,4-*b*]-1,3,4-thiadiazines. *IlFarmaco* **2001**, *56*, 919–927.
16. Turan-Zitouni, G.; Kaplancikli, Z.A.; Erol, K.; Kilic, F.S. Synthesis and analgesic activity of some triazoles and triazolothiadiazines. *Il Farmaco* **1999**, *54*, 218–223.
17. Holla, B.S.; Gonsalves, R.; Shenoy, S. Studies on some N-bridged heterocycles derived from bis-[4-amino-5-mercapto-1,2,4-triazol-3-yl] alkanes. *Il Farmaco* **1998**, *53*, 574–578.
18. Holla, B.S.; Sarojini, B.; Rao, S.B.; Akberali, P.M.; Kumari, N.S.; Shetty, V. Synthesis of some halogen-containing 1,2,4-triazolo-1,3,4-thiadiazines and their antibacterial and anticancer screening studies — Part I*[1]. *Il Farmaco* **2001**, *56*, 565–570.
19. Adlard, P.A.; Cherny, R.A.; Finkelstein, D.I.; Gautier, E.; Robb, E.; Cortes, M.; Volitakis, I.; Liu, X.; Smith, J.P.; Perez, K.; Laughton, K.; Li, Q.X.; Charman, S.A.; Nicolazzo, J.A.; Wilkins, S.; Deleva, K.; Lynch, T.; Kok, G.; Ritchie, C W.; Tanzi, R.E.; Cappai, R.; Masters, C.L.; Barnham, K.J.; Bush, A.I. Rapid restoration of cognition in Alzheimer's transgenic mice with 8-hydroxy quinoline analogs is associated with decreased interstitial Aβ , Abeta. *Neuron* **2008**, *59*, 43–55.
20. Thompson, P.E.; Reinertson, J.W. Chemotherapy of amebic hepatitis in hamsters with emetine, chloroquine, amodiaquin (camoquin), quinacrine and other drugs. *Am. J. Trop. Med. Hyg.* **1951**, *31*, 707–717.
21. Oien, N.L.; Brideau, R.J.; Hopkins, T.A.; Wieber, J.L.; Knechtel, M.L.; Shelly, J.A.; Anstadt, R.A.; Wells, P.A.; Poorman, R.A.; Huang, A.; Vaillancourt, V.A.; Clayton, T.L.; Tucker, J.A.; Wathen, M.W. Broad-spectrum antiherpes activities of 4-hydroxyquinoline carboxamides, a novel class of herpesvirus polymerase inhibitors. *Antimicrob. Agents Chemother*. **2002**, *46*, 724–730.
22. Ji, H.F.; Zhang, H.Y. A new strategy to combat Alzheimer's disease. Combining radical-scavenging potential with metal-protein-attenuating ability in one molecule. *Bioorg. Med. Chem. Lett.* **2005**, *15*, 21–24.
23. Peng, R.; Wang, F.; Sha, Y. Synthesis of 5-dialkyl(aryl)aminomethyl-8-hydroxyquinoline dansylates as selective fluorescent sensors for Fe^{3+}. *Molecules* **2007**, *12*, 1191–1201.
24. Patel, H.S.; Oza, K. K. Synthesis, characterization and antimicrobial activity of metal chelate of 5-[1(h)-benzotriazole methylene]-8-quinolinol. *E-Journal of Chem.* **2009**, *6(2)*, 371–376.
25. Maurya, R.C.; Patel, P.; Rajput, S. Synthesis and characterization of N-(o-Vanillinidene)-p-anisidine and N,N′-bis(o-vanillinidene)ethylenediamine and their metal complexes. *Synth. React. Inorg. Met.-Org. Chem.* **2003**, *33*, 817–836.
26. Joshi, J.D.; Sharma, S.; Patel, G.; Vora, J.J. Synthesis And characterization of nickel(II), zinc(II), and cadmium(II) mixed-ligand complexes with 2,2′-bipyridylamine and phenols. *Synth. React. Inorg. Met.-Org. Chem.,* **2002**, *32*, 1729–1741.
27. Vogel, A.I. *A Textbook of Practical Organic Chemistry,* 5th edn.; Longman: London, 1989.
28. Vogel, A.I. *A Textbook of Quantitative Inorganic Analysis,* 4th edn.; ELBS and Longman: London, 1978.
29. Shah, T.B.; Dixit, B.C.; Dixit, R. B. Novel polymeric chelates of 8-hydroxyquinoline-dimethylolacetone. *J. Therm. Anal. Calor.* **2008**, *92*, 505–512.
30. Bayrak, H.; Demiras, A.; Demirbas, N.; Karaoglu, S.A. Synthesis of some new 1,2,4-triazoles starting from isonicotinic acid hydrazide and evaluation of their antimicrobial activities. *Euro. J. Med. Chem.* **2009**, *44*, 4362–4366.
31. Kharadi, G.J.; Patel, K.D. Antibacterial, spectral and thermal aspects of drug based-Cu(II) mixed ligand complexes. *Appl. Organomet. Chem,* **2009**, *23*, 391–397.
32. Burckhalter, J.H.; Leib, R.I. Amino-and chloromethylation of 8-quinolinol. mechanism of preponderant ortho substitution in phenols under Mannich conditions. *J. Org. Chem.* **1961**, *26*, 4078–4083.
33. Charles, R.G.; Freiser, H.; Friedel, R.; Hilliard, L. E.; Johnston, W. D. Infrared absorption spectra of metal chelates derived from 8-hydroxyquinoline, 2-methyl-8-hydroxyquinoline, and 4-methyl-8-hydroxyquinoline. *Spectrochim. Acta.* **1956**, *8*, 1–8.
34. Nakamoto, N. *Infrared Spectra and Raman Spectra of Inorganic and Coordination Compounds;* John Wiley & Sons: New York, 1978.
35. Almajan, G.L.; Barbuceanu, S.F.; Saramet, I.; Draghici, C. New 6-amino-[1,2,4]triazolo[3,4-b][1,3,4]thiadiazines and [1,2,4]triazolo[3,4-b] [1,3,4]thiadiazin-6-ones: Synthesis, characterization and antibacterial activity evaluation. *Euro. J. Med. Chem.* **2010**, *45*, 3191–3195.
36. Pansuriya, P.B.; Patel, M.N. Synthesis, spectral, thermal, DNA interaction and antimicrobial properties of novel Cu(II) heterochelates. *Appl. Organomet. Chem.* **2007**, *21*, 739–749.
37. Alafandy, M.; Willem, R.; Mahieu, B.; Alturky, M.; Gielen, M.; Biesemans, M.; Legros, F.; Camu, F.; Kauffmann, J.M. Preparation and characterization of bis(8-quinolinato)tin(II). *Inorg. Chim. Acta.* **1997**, *255*, 175–179.
38. Kidri, J.; Hadi, D.; Kocjan, D.; Rutar, V. ^{1}H and ^{13}C NMR study of 8-hydroxyquinoline and some of its 5-substituted analogues. *Org. Magnet. Reson.* **2004**, *15*, 280–284.
39. Iggo, J.A. *NMR Spectroscopy in Inorganic Chemistry;* Oxford University Press: New York, 1999.
40. Reddy, K.M.; Halli, H.P.; Hiremath, A.C. Co(II), Ni(II) and Cu(II) Complexes with Aniline Schiff's Bases. *J. Indian Chem. Soc.* **1994**, *71*, 751–759.
41. Kriza, A.; Pricop, L.; Meghean, A.; Stanica, N. Template synthesis of Cr(III), Co(II), Ni(II), Cu(II) and Cd(II) complexes with a tetradentate Schiff base, glyoxilidene-2-aminoethylpyridine. *J. Indian Chem. Soc.* **2001**, *78*, 448–452.
42. Dixit, R.B.; Vanparia, S.F.; Patel, T.S.; Jagani, C.L.; Doshi, H.V.; Dixit, B.C. Synthesis and antimicrobial activities of sulfonohydrazide-substituted 8-hydroxyquinoline derivative and its oxinates. *Appl. Organomet. Chem.* **2010**, *24*, 408–413.
43. Raman, N.; Thangaraja, C.; Raja, S.J. Mixed ligand transition metal(II) complexes of Knoevenagelcondensate-bB>-ketoesters with 1,2-diaminobenzene:synthesis, structural characterization, electrochemical behaviour andantimicrobial study. *Indian J. Chem., Sect. A* **2005**, *44A*, 693–699.
44. Bailer, J.C.; Judd, M.L.; McLean, J. WADC, Technical Reports Part-II **1959**, 116–145, 51–58.
45. Cotton, F.A.; Wilkinson, G. *Advanced Inorganic Chemistry*, 5th edn.; Wiley Interscience: New York, **1988**.
46. Freeman, E.S.; Carroll, B. The application of thermoanalytical techniques to reaction kinetics: the thermogravimetric evaluation of the kinetics of the decomposition of calcium oxalate monohydrate. *J. Phys. Chem.* **1958**, *62*, 394–397.
47. Modi, C.K.; Patel, S.H.; Patel, M. N. Transition metal complexes with uninegative bidentate Schiff base synthetic, thermal, spectroscopic and coordination aspects. *J. Therm. Anal. Calorim.*, **2007**, *87*, 441–448.
48. El-Zaria, M.E. Spectrophotometric study of the charge transfer complexation of some porphyrin derivatives as electron donors with tetracyanoethylene. *Spectrochim. Acta A* **2008**, *69*, 216–221.
49. Parekh, H.M.; Panchal, P.K.; Patel, M.N. Transition metal(II) ions with dinegative tetradentate schiff base Synthetic, thermal, spectroscopic and coordination aspects. *J. Therm. Anal. Calorim.* **2006**, *86*, 803–807.
50. Jani, D.H.; Patel, H.S.; Keharia, H.; Modi, C.K. Novel drug-based Fe(III) heterochelates: synthetic, spectroscopic, thermal and in-vitro antibacterial significance. *Appl. Organomet. Chem.* **2010**, *24*, 99–111.
51. Parekh, H.M.; Pansuriya, P.B.; Patel, M. N. Characterization and antifungal study of genuine oxovanadium(IV) mixed-ligand complexes with Schiff bases. *Polish J. Chem.*, **2005**, *79*, 1843–1851.

52. Chohan, Z.H.; Khan, K.M.; Supuran C. T. Synthesis of antibacterial and antifungal cobalt(II), copper(II), nickel(II) and zinc(II) complexes with bis-(1,1′-disubstituted ferrocenyl)thiocarbohydrazone and bis-(1,1′-disubstituted ferrocenyl)carbohydrazone. *Appl. Organomet. Chem.* **2004**, *18*, 305–310.
53. Heath, O.V.S.; Clark, J.E. Chelating agents as growth substances. *Nature*, **1957**, *178*, 600–601.
54. Nair, R.; Shah, A.; Baluja, S.; Chanda, S. Synthesis and antibacterial activity of some Schiff base complexes. *J. Serb. Chem. Soc*. **2006**, *71*, 733–744.
55. Patel, M.N.; Chhasatia, M.R.; Gandhi, D.S. DNA-interaction and *in vitro* antimicrobial studies of some mixed-ligand complexes of cobalt(II) with fluoroquinolone antibacterial agent ciprofloxacin and some neutral bidentate ligands. *Bioorg. Med. Chem. Lett.* **2009**, *19*, 2870–2873.